ac driving amplitude dependent systematic error in scanning Kelvin probe microscope measurements: Detection and correction

Yan Wu and Mark A. Shannon
Department of Mechanical and Industrial Engineering, University of Illinois at Urbana-Champaign, 1206 West Green Street, Urbana, Illinois 61801

(Received 18 January 2006; accepted 19 March 2006; published online 21 April 2006)

The dependence of the contact potential difference (CPD) reading on the ac driving amplitude in scanning Kelvin probe microscope (SKPM) hinders researchers from quantifying true material properties. We show theoretically and demonstrate experimentally that an ac driving amplitude dependence in the SKPM measurement can come from a systematic error, and it is common for all tip sample systems as long as there is a nonzero tracking error in the feedback control loop of the instrument. We further propose a methodology to detect and to correct the ac driving amplitude dependent systematic error in SKPM measurements. The true contact potential difference can be found by applying a linear regression to the measured CPD versus one over ac driving amplitude data. Two scenarios are studied: (a) when the surface being scanned by SKPM is not semiconducting and there is an ac driving amplitude dependent systematic error; (b) when a semiconductor surface is probed and asymmetric band bending occurs when the systematic error is present. Experiments are conducted using a commercial SKPM and CPD measurement results of two systems: platinum-iridium/gap/gold and platinum-iridium/gap/thermal oxide/silicon are discussed. © *2006 American Institute of Physics.* [DOI: 10.1063/1.2195104]

I. INTRODUCTION

The scanning Kelvin probe microscope[1] (SKPM) is a modified version of an atomic force microscope (AFM) that can map the differences in voltage potential between the tip of the AFM probe and the sample, accounting for the topography of the surface. The contact potential difference (CPD) detected by SKPM is the sum of the work function difference of the tip-sample system and the surface potential of the sample. SKPM is a powerful tool to characterize materials for electrical properties in the micro- to nanometer scale. Applications of SKPM include the electrical failure analysis of integrated circuits, detection of trapped charges, heterojunction imaging, mapping of the relative strength and direction of an electric polarization, and read/write the electrical charge.[2] In some of these applications, a CPD mapping showing the relative potential difference within an image is adequate. In other applications, such as surface photovoltage measurement,[2,3] dopant profiling,[4] and work function mapping,[5] researchers are interested in quantifying the CPD between the tip and the sample. We are interested in extending the use of SKPM to measure the CPD of surfaces that are functionalized with moieties with dipole charges at different end groups. In particular, we are interested in extracting the surface potential of a gold surface functionalized with thiol-terminated moieties and silicon-silicon oxide surfaces terminated with silanol compounds, which are surface functionalized materials being studied in water-constituent interactions. In many of these applications, the absolute value of the CPD between the tip and the sample at every pixel of an image is the measurement target. The overall goal for absolute CPD measurements is to extract the change in the surface potential due the presence of surface charges and/or dipoles. A common problem encountered, however, is that the CPD can be within a systematic error that occurs when the ac amplitude is imposed on the SKPM measurements, which is often the case for surface functionalized dipoles.

Figure 1 shows a schematic view of a typical SKPM setup. The AFM scans the sample with two passes. On the first pass, the standard tapping mode determines the sample's topography. On the second pass, or the SKPM scan, as illustrated in Fig. 1, the tip is lifted above the tapping mode scan height to a specified lift height. During the SKPM scan, an alternating voltage $V_{\mathrm{ac}} \sin(\omega_a t)$ at the cantilever resonant frequency ω_a and a dc bias V_{dc} are applied to the conductive AFM tip in order to induce a cantilever vibration due to the periodical electrostatic force between the tip and the sample. The cantilever vibration amplitude at ω_a is proportional to the potential difference between the tip potential, V_{dc}, and the surface potential of the sample. The contact potential difference of a tip-sample system can be measured by adjusting the dc bias V_{dc} using a feedback loop until the cantilever vibration amplitude at ω_a is nullified. Theoretically, the measured value of the CPD should depend only on the material properties of the sample. Practically, however, SKPM readings have been affected by several operational parameters such as the tip-sample distance g in the SKPM scan,[6–8] the drive phase φ that compensates the phase lag θ between the cantilever excitation signal and the cantilever response signal,[9] and the ac driving amplitude V_{ac}[4,8,10–12]

The dependence of SKPM readings on operational parameters is problematic in those applications that rely on quantitative CPD values to characterize material properties. The mechanisms for the dependence of the SKPM readings on the first two operational parameters (tip-sample distance g

0034-6748/2006/77(4)/043711/9/$23.00 © 2006 American Institute of Physics

Downloaded 04 May 2006 to 130.126.178.112. Redistribution subject to AIP license or copyright, see http://rsi.aip.org/rsi/copyright.jsp

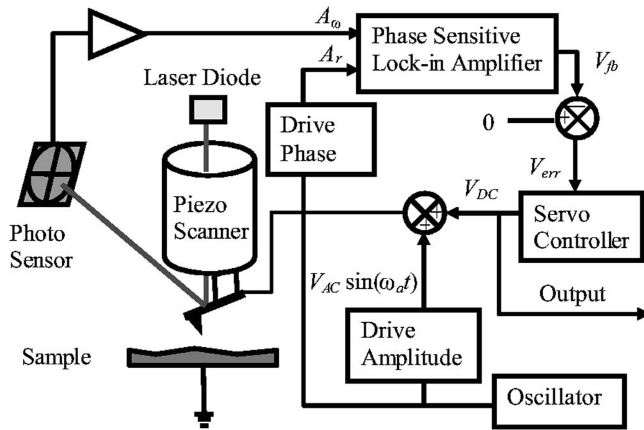

FIG. 1. A simplified block diagram of the SKPM scan of a scanning Kelvin microscope. The AFM probe is biased by an alternating voltage $V=V_{\mathrm{dc}}+V_{\mathrm{ac}}\sin(\omega_a t)$. A lock-in amplifier detects the cantilever deflection signal at frequency ω_a. The dc component of the applied voltage is adjusted by a servo controller until the vibration of the probe tip at frequency ω_a is zero.

and drive phase φ) are well studied,[6,9] and guidelines for adjusting these parameters to improve the measurement resolution and sensitivity were suggested. Leng and Williams[10] proposed that the asymmetric carrier response to the external field leads to an ac driving amplitude dependent SKPM reading when a semiconductor surface is being scanned. Due to the asymmetric nature of the space charge response in a semiconductor surface to an applied electric field, i.e., the surface potential change in depletion much greater than that in accumulation, an alternating field results in a net surface potential change. The magnitude of this net surface potential change depends on the magnitude of the ac electric field since the greater the applied alternating electric field is, the more asymmetric the response of the semiconductor surface will be. For this reason, others[8,11] have proposed that a small V_{ac} (compared to the semiconductor band gap) will help to reveal the true CPD between the tip and the sample. Arakawa *et al.*[12] reported that reducing the driving amplitude may lead to a loss of voltage signal to noise resolution in SKPM measurements. In our research, we find that the V_{ac} dependent reading is not unique to semiconductor samples. As we shall demonstrate later, the tracking error in the feedback control loop of typical SKPM systems can also cause an ac driving amplitude dependent shift in SKPM measurements that causes a systematic error, which skews the CPD estimate. The uncertainty of the SKPM measurement due to this systematic error increases as the ac driving amplitude decreases. When the ac driving amplitude is small and a systematic error is present, the measurement results show an even greater dependence on the ac driving amplitude.

For these cases, in order to correctly interpret the CPD reading measured by SKPM, especially in the applications where the absolute value of CPD is being sought, it is important to identify the cause of the ac driving amplitude dependence of the SKPM measurements. The purpose of the current work is to provide a methodology to detect and correct an ac driving amplitude dependent systematic error in SKPM measurements, thus permitting the actual CPD value due to the material property of the sample to be determined.

Two scenarios are studied when a V_{ac} dependent systematic error is present: (a) when the surface is on a semiconductor base and asymmetric band bending occurs and (b) when the surface being scanned by SKPM is not semiconducting (metallic and/or dielectric). A theoretical model that captures this systematic error is developed, and experimental data is presented to demonstrate the errors induced by V_{ac}. The proposed methodology to separate the systematic error from actual CPD values in SKPM measurements is applied to the experimental data, and the results are discussed.

II. THEORY

A. The driving amplitude V_{ac} dependent systematic error

During the SKPM scan, the tip is lifted above the sample to a specified scan height. When a voltage is applied between the sample and the metal cantilever probe, the electrostatic force acting on the tip can be given by

$$F=f(g)(V-V_c)^2, \tag{1}$$

where $f(g)$ (units of F/m) represents the capacitive coupling between the tip and the sample. The functional form of $f(g)$ depends in a complicated fashion upon the tip geometry and tip-sample distance[13] g. The contact potential difference V_c is the measurement target. It can be expressed using the work function of the probe W_P (eV) and sample W_1 (eV) and the surface potential of the sample ϕ_1 (volt), such that

$$V_c=\phi_1+(W_P-W_1)/e. \tag{2}$$

When the applied voltage has an ac component and a dc component,

$$V=V_{\mathrm{dc}}+V_{\mathrm{ac}}\sin(\omega_a t), \tag{3}$$

and inserting Eq. (3) into Eq. (1) yields

$$F=f(g)\left[(V_{\mathrm{dc}}-V_c)^2+\frac{V_{\mathrm{ac}}{}^2}{2}+2V_{\mathrm{ac}}(V_{\mathrm{dc}}-V_c)\sin(\omega_a t)-\frac{1}{2}V_{\mathrm{ac}}\cos(2\omega_a t)\right]. \tag{4}$$

Equation (4) shows that the electrostatic force acting on the tip has two steady-state components (first two terms), as well as oscillating components (last two terms) at ω_a and $2\omega_a$. The oscillation of the cantilever probe induced by this electrostatic force is detected from the optical deflection of a laser off the cantilever probe using a position sensitive detector or a laser interferometer. A phase sensitive lock-in amplifier selectively detects the amplitude of the tip oscillation at frequency ω_a. The measured oscillation signal amplitude at frequency ω_a can be expressed as

$$A_\omega=Kf(g)V_{\mathrm{ac}}(V_{\mathrm{dc}}-V_c), \tag{5}$$

where K is a constant that is determined by the mechanical property of the cantilever. In the ideal situation, the dc bias voltage is adjusted by a servo controller until the vibration of the probe at ω_a is absolutely zero. At this point, Eq. (5) gives

Downloaded 04 May 2006 to 130.126.178.112. Redistribution subject to AIP license or copyright, see http://rsi.aip.org/rsi/copyright.jsp

$$V_{dc} = V_c = \phi_1 + (W_P - W_1)/e, \tag{6}$$

and the dc bias voltage is used as the output signal of the SKPM measurement.

The above analysis is based on the ideal situation that the feedback loop of the servo controller nulls the cantilever vibration completely to zero. In reality, however, there is a tracking error between the target response and the actual response in the control loop. The magnitude of this tracking error depends on the servo controller setup. Assuming this tracking error signal corresponds to a voltage, V_{err}, and the target response to the controller is zero, we have

$$0 - V_{fb} = -\beta A_\omega A_r \cos(\theta - \varphi) = V_{err}. \tag{7}$$

In this equation, V_{fb} is the actual response that is used as the feedback signal to the controller. The feedback signal V_{fb} is determined by the gain of the lock-in amplifier β, the amplitude of the reference signal A_r, and the phase difference between the reference signal and the cantilever vibration signal, θ-φ. Substituting Eq. (5) into Eq. (7), we find that the output, V_{dc}, of SKPM in the presence of a nonzero tracking error V_{err} can be expressed as

$$V_{dc} = \frac{m}{V_{ac}} + V_c, \quad m = \frac{-V_{err}}{Kf(g)\beta A_r \cos(\theta - \varphi)}. \tag{8}$$

The first term of Eq. (8) indicates that the measured output of SKPM contains a systematic error offsetting the measurement target V_c. Note that this systematic error depends inversely on the driving amplitude V_{ac}.

The driving amplitude V_{ac} dependent systematic error in Eq. (8) should not be confused with the V_{ac} dependent V_c signal for semiconductor samples. For a semiconductor surface with a space charge layer, V_c can be expressed as

$$V_c = V_s(Q_s) + (W_p - W_s)/e, \tag{9}$$

where V_s (volt) and Q_s (C/cm^2) are the surface potential and the space charge density of the semiconductor, respectively. W_P (eV) and W_s (eV) are the work functions of the probe and the semiconductor, respectively.

When there is an alternating electric field at the semiconductor surface, Q_s can be expressed as

$$Q_s(t) = Q_f + \Delta Q(t), \tag{10}$$

where Q_f is a field-independent fixed space charge Q_f. The time dependent part $\Delta Q(t)$ is due to the charge carrier response to the alternating electric field. Assuming that the charge carrier response due to the surface states can be ignored, i.e., the semiconductor surface is not pinned by surface states, the time dependent charge ΔQ can be expressed as

$$\Delta Q = V_{ac} \sin(\omega_a t) C(g), \tag{11}$$

where $C(g)$ is an effective capacitance between tip and sample. Like $f(g)$ in Eq. (1), $C(g)$ is determined by the tip geometry and the tip-sample distance g. As g *decreases*, $C(g)$ increases. The functional form of $C(g)$ has been of great interest for researchers who specialized in the field of scanning capacitance microscopy[14,15] (SCM) and is not the primary focus here. The V_{ac} dependent V_c signal for semiconductor samples under an alternation electric field can be expressed as

$$V_c = V_s[Q_f + V_{ac} \sin(\omega_a t) C(g)] + (W_p - W_s)/e. \tag{12}$$

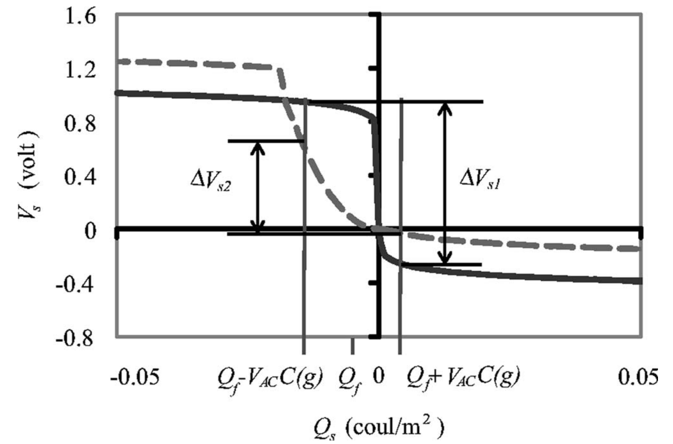

FIG. 2. The surface potential V_s is plotted as a function of space charge density Q_s for uniformly doped p-type semiconductor, illustrating the effect of low doping (1×10^{15} cm^{-3} and solid line) and high doping (1×10^{19} cm^{-3}, dashed line) on V_s. With the same Q_f and same magnitude of ΔQ as shown in this figure, there is a greater change of V_s for the lightly doped sample (ΔV_{s1}) than the heavily doped sample (ΔV_{s2}).

The relationship between V_s and Q_s is well studied for uniformly doped semiconductor surfaces.[16] Figure 2 illustrated the dependence of V_s on Q_f, V_{ac}, and $C(g)$ for uniformly doped p-type semiconductor surfaces with two different doping levels (1×10^{15} and 1×10^{19} cm^{-3}). In Fig. 2, the fixed charge Q_f falls in the depletion region for both samples. With the same Q_f and same magnitude of ΔQ, there is a greater change of V_s for the lightly doped sample (solid line in Fig. 2) than for the heavily doped sample (dashed line Fig. 2). The lightly doped sample shows a greater dependence of V_s on ΔQ because for the same amount of ΔQ, the total space charge Q_s swings from accumulation to inversion, whereas Q_s only changes from an accumulation to a *partial* depletion for the heavily doped sample. For a pinned semiconductor surface, the change in electric field is blocked by the charge in the surface states; thus its surface potential remains unchanged. In general, assuming that the semiconductor surface is not pinned by the surface state and the space charge response is fast enough to follow the alternating electric field, the conditions for a detectable surface potential change to occur include (a) a small fixed space charge Q_f that falls in either a weak depletion or a weak accumulation region and (b) a large driving V_{ac} or small tip sample distance g such that the $\Delta Q(t)$, which is determined by the product of V_{ac} and $C(g)$, is large enough to cause $Q_s(t)$ to swing from accumulation to inversion.

The V_{ac} dependence caused by the asymmetric band bending occurs only for semiconductor samples at particular conditions. The condition for the driving amplitude V_{ac} dependent systematic error to occur is a nonzero tracking error in the control loop, which is common for most instruments and is not restricted to certain types of samples. In the case when both driving amplitude dependent systematic error and semiconductor surface nature originated V_{ac} dependence are

Downloaded 04 May 2006 to 130.126.178.112. Redistribution subject to AIP license or copyright, see http://rsi.aip.org/rsi/copyright.jsp

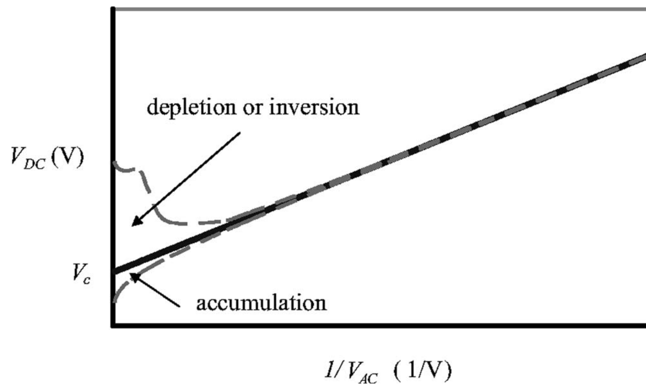

FIG. 3. The relationship between SKPM output V_{dc} and inverse driving amplitude $1/V_{ac}$, when a nonzero tracking error in the feedback loop exists. The solid line represents the case when the surface being scanned by SKPM is not semiconducting and there is an ac driving amplitude dependent systematic error. The dashed line represents the case when a uniformly doped p-type semiconductor surface is probed, and an asymmetric band bending occurs concurrently when the systematic error is present.

present, the measured output of SKPM can be expressed as

$$V_{dc} = \frac{m}{V_{ac}} + V_s[Q_f + V_{ac}\sin(\omega_a t)C(g)] + (W_p - W_s)/e,$$

$$m = \frac{-V_{err}}{Kf(g)\beta A_r \cos(\theta - \varphi)}. \tag{13}$$

B. Methodology to separate actual CPD from systematic error in SKPM

In order to identify the V_{ac} dependent systematic error, we need to understand the extrinsic response of the system for different intrinsic material types. To determine the extrinsic response of the system, generally speaking, the gain of the lock-in amplifier β and the amplitude of the reference signal A_r do not depend on the cantilever vibration amplitude A_ω. For a given tip-sample system with a fixed tip-sample distance, Eq. (5) indicates that the A_ω signal is linearly proportional to V_{ac}. If the phase lag θ (between the cantilever excitation signal and the cantilever response signal) remains nearly the same as V_{ac} changes, the feedback signal V_{fb} in Eq. (7) is linearly proportional to V_{ac} for a fixed drive phase φ. The tracking error V_{err} depends on the settings on the servo controller. Assuming that the V_{err} is constant for a particular system, Eq. (8) shows that the output V_{dc} is a linear function with respect to $1/V_{ac}$. To detect the V_{ac} dependent systematic error in SKPM readings, a V_{dc} vs $1/V_{ac}$ curve can be plotted. If V_{dc} is a linear function of $1/V_{ac}$ as the solid line in Fig. 3, the systematic error varies with slope m in Eq. (8). Furthermore, the true V_c signal in Eq. (8) can be found from the y intercept of the plot, as shown in Fig. 3 (solid line). Thus, the true contact potential difference measured by SKPM can be separated from the systematic error by a linear regression.

The intrinsic response depends on the material type. For instance, when the V_{ac} dependence due to an asymmetric band bending of semiconductor surfaces occurs concurrently with a V_{ac} dependent systematic error, Eq. (13) indicates that the proportion of the systematic error increases in the total output as V_{ac} decreases. A decrease in V_{ac} leads to a smaller $\Delta Q(t)$, thus a smaller change in the surface potential V_s in the total output. The area within the dashed lines in Fig. 3 shows the possible output of V_{dc} as a function of $1/V_{ac}$ for uniformly doped p-type semiconductor samples at a fixed tip-sample distance. The solid line in this case represents the sum of the systematic error, the surface potential due to a fixed space charge Q_f, and the work function difference between the tip and the semiconductor sample $(W_p - W_s)/e$. When V_{ac} is small enough, the dashed lines fall on top of the solid line in Fig. 3, indicating that the dominant cause of the V_{ac} dependent output is the systematic error. In this region, the output V_{dc} has a linear relationship with respect to $1/V_{ac}$. However, at high V_{ac}, when the space charge is large enough, a linear relationship between V_{dc} and $1/V_{ac}$ no longer exists, as illustrated by the dashed lines in Fig. 3. The output may fall at any point within the dashed lines in this region, depending on the oscillating bias, because the surface of the sample reaches accumulation when the tip is under a positive bias, while under a negative bias it goes into depletion or even potentially into inversion. We propose a practical criterion to determine how small V_{ac} needs to be such that no significant change in V_s occurs, such that

$$\sigma(g) = \frac{\varepsilon_0 V_{ac}}{g} \leqslant \frac{1}{2}|Q_{d,\max}|, \tag{14}$$

where $\sigma(g)$ is the maximum surface charge density at the semiconductor surface due to the oscillating electric field at tip-sample distance g, ε_0 is the permittivity in vacuum, and $Q_{d,\max}$ is the maximum depletion charge per unit area at the semiconductor surface. When the magnitude of the space charge is less than half of the maximum depletion charge, the dominate cause of a V_{ac} dependent output is the systematic error rather than the oscillation in the surface potential. In this region, the same methodology to detect and correct the systematic error proposed previously can be applied, as shown in Fig. 3. The y intercept of the plot in this case is the sum of the surface potential due to a fixed space charge Q_f and the work function difference between the tip and the semiconductor sample $(W_p - W_s)/e$.

Practically, there is another restriction to the V_{ac} region to apply the proposed methodology. The analysis above is based on the assumption that the feedback signal V_{fb} in Eq. (7) is linearly proportional to V_{ac}, such that the coefficients of the parameters in m in Eq. (13) are constant as V_{ac} changes. However, the linear relationship between V_{fb} and V_{ac} is only approximate over a certain range of V_{ac} since the phase lag θ and tip-sample distance g are also dependent on the driving amplitude V_{ac}. This dependence is due to a steady-state force in the electrostatic force, such that

$$F_{dc} = f(g)\left[(V_{dc} - V_c)^2 + \frac{V_{ac}{}^2}{2}\right], \tag{15}$$

which acts to displace the AFM tip. Even if V_{dc} equals V_c, the dc component of the electrostatic force is not zero, but proportional to the square of the driving amplitude V_{ac}. In the SKPM scan, the cantilever is lifted above the trajectory of the cantilever in the topography scan to a user specified height Z_L. The tip-sample distance g is determined by the

Downloaded 04 May 2006 to 130.126.178.112. Redistribution subject to AIP license or copyright, see http://rsi.aip.org/rsi/copyright.jsp

tapping mode scan height Z_T, the lift height Z_L, and the bending of the cantilever due to F_{dc}. Increasing V_{ac} will increase the bending of the cantilever and change the average tip-sample distance g. Since the effective spring constant of the tip-sample interaction depends on F_{dc}, changes in the V_{ac} also result in changes in the phase lag θ between the cantilever excitation signal and the response signal. The proposed methodology to recover the true contact potential difference measured by SKPM requires measuring V_{dc} with various V_{ac}. Depending on the particular experiment, the change in the tip-sample distance g and the phase lag θ may or may not be a strong function of V_{ac}. In general, a small magnitude range of V_{ac} is beneficial because F_{dc} increases quadratically with V_{ac}. To find the range over which the feedback signal to the controller V_{fb} is approximately linear with respect to the V_{ac}, the open loop V_{fb} response to V_{ac} needs to be measured.

In summary, the methodology to detect and correct the driving amplitude dependent systematic error in SKPM measurements includes four steps. First, the sample topography is scanned in the normal tapping mode, and the tapping mode scan height Z_T is estimated by the product of the tapping mode amplitude sensitivity and the amplitude set point. Second, the sample is scanned in the SKPM mode, while the AFM tip is lift up above the trajectory of the cantilever in the topography scan to a user specified lift height Z_L. The tip-sample distance can be estimated by the sum of Z_L and Z_T (the bending of the cantilever due to F_{dc} is neglected here). Third, the linear region for the open loop V_{fb} to the V_{ac} response is found. This V_{ac} region determines the linear range over which the close loop V_{dc} response is to be measured in the next step because the proposed methodology is based on the assumption that the V_{fb} to the V_{ac} response is linear. For a semiconductor sample, V_{ac} is also subjected to the restriction expressed in Eq. (14), which gives an estimate of the maximum V_{ac} that can be used without a significant change in the surface potential for a given tip-sample distance (estimated in step 2). Finally, the closed loop V_{dc} response as a function of V_{ac} is measured, and a V_{dc} vs $1/V_{ac}$ curve is plotted. If V_{dc} is a linear function of $1/V_{ac}$, it suggests that there is a V_{ac} dependent systematic error as described in this article in SKPM readings. The actual contact potential difference being sought with SKPM can be found from the intercept on the y axis in this plot.

The methodology presented in this article is for detecting and correcting the ac driving amplitude dependent systematic error in order to recover the true CPD. Special precautions are needed to interpret the recovered CPD value when applying this methodology on nonhomogeneous samples, where the CPD varies with location. In this case, the recovered CPD value on a particular location is not determined solely by the area directly under the tip, but rather is a function of the CPDs of various locations as described in the article of Jacobs *et al.*[6] The form of this function is subjected to the tip-sample distance, the tip geometry, and especially the effect of the cantilever capacitance pickup.[17,18] For example, when the cantilever of an AFM probe reaches over areas with a potential differing from the one directly under the tip, the recovered CPD value may contain a shift from the areas under the cantilever since the cantilever is also a part of the sensing device in the SKPM measurement.[18]

III. EXPERIMENTS

The experiments are conducted using a commercial AFM (NanoScope® IV Dimension 3100™ with Extender™ Electronics Module, Veeco, USA). The AFM probes are coated with platinum-iridium (SCM-PIT™, Veeco, USA). Two types of samples are tested: gold thin films (nonsemiconducting sample) and uniformly doped p-type silicon substrates (semiconducting sample) with a thin thermal silicon oxide passivation layer. In order to avoid the complication in the experimental results due to the local variation of the sample's surface potential, we used samples with surfaces that are homogenous over dimensions much larger than the AFM probe size.

The gold thin films are deposited by a reactive sputtering at room temperature on silicon wafers of 100 mm in diameter. There is 1-μm-thick thermal oxide on the silicon to electrically isolate the Au from the Si substrate. The gold thin film is deposited at a power of 300 W at a pressure of 1.9×10^{-3} mTorr. The total thickness of the deposited gold film is estimated to be 1 μm. An electrical contact is made directly via soldering at the surface of the gold thin film sample.

Double-sided polished p-type silicon wafers with a resistivity of 3–6 Ω cm are first doped at 950 °C using a solid boron nitride diffusion source. A thermal silicon oxide is grown on both sides at 1100 °C in oxygen for 30 min. The oxide film is then annealed at 940 °C in nitrogen for 20 min. The thickness of the thermal oxide as measured by an elipsometer is 98 nm. The purpose of growing a thin thermal oxide on top of the silicon substrate is to reduce the surface states at the silicon surface.[19] The oxide at the backside of the wafer is striped, and a layer of aluminum with a thickness of 150 nm is deposited on the back side using a dc magnetron sputtering. The wafer is then annealed at 450 °C so that an Ohmic contact is formed at the aluminum/p-plus silicon junction on the backside of the wafer. During testing, the sample is held by a vacuum chuck, and the electrical connection to the ground of the instrument is made via a grounded sample chuck.

For both types of samples, the AFM uses two passes to scan the sample. In the first pass, the surface topography of a single line is acquired using the normal tapping mode scan. The scan height of the cantilever Z_T in the tapping mode can be estimated by the product of the amplitude sensitivity of the cantilever and the amplitude set point voltage. In the second pass (SKPM scan) that immediately follows the first pass over the same line, the AFM probe is lifted above the tapping mode scan height to a user specified height Z_L. A biased oscillation voltage with the cantilever resonance frequency ω_a is applied to the conductive probe. A phase sensitive lock-in amplifier selectively detects the amplitude of the tip oscillation at frequency ω_a. A servo controller automatically adjusts the dc bias to null the probe oscillation at the frequency ω_a. The dc bias voltage V_{dc} is used as the output signal of the SKPM measurement. The drive phase φ

Downloaded 04 May 2006 to 130.126.178.112. Redistribution subject to AIP license or copyright, see http://rsi.aip.org/rsi/copyright.jsp

TABLE I. Run time parameters of the experiments.

Experiment	Bias (V)	Cantilever resonance frequency, ω_a (kHz)	Drive phase, φ (degree)	Amplitude sensitivity (nm/V)	Amplitude set point (V)	Lift height Z_L (nm)	Tip-sample distance[a] g (nm)
I	1	64.3	−87.0	41.8	1.353	5	61.6
II	0 to 1	63.5	−87.0	26.6	1.198	0	31.8
III	0	64.2	−85.4	39.4	1.174	5	51.3

[a]The tip-sample distance is estimated by the sum of the lift height Z_L and tapping mode scan height Z_T, i.e, the product of amplitude sensitivity and amplitude set point.

that compensates the phase lag θ between the cantilever excitation signal and the cantilever response signal is fine tuned to maximize the output of the lock-in amplifier according to the procedure outlined by Jacobs *et al.*[9] By setting the gains in the servo controller to be zero, the control loop can be switched to an open state and the feedback signal V_{fb} can be monitored using the phase data channel.[20] The unit of V_{fb} is recorded as an arbitrary unit since the information of the real unit of V_{fb} data is unavailable from the instrument being used. When the control loop is open, the system keeps V_{dc} at 0 V. To find out within what range the feedback signal to the controller V_{fb} is approximately linear with respect to the driving amplitude V_{ac}, the response of V_{fb} as a function of V_{ac} is measured with an open feedback control loop. After that, the control loop is closed by setting the gains of the feedback loop with a manufacture recommended value, and the response of V_{dc} as a function of V_{ac} is measured for each type of samples.

Three experiments are performed. Detailed run time parameters for each experiment are listed in Table I. All the measurements are performed in air. For the gold thin film sample, a dc power supply (Protek 300) is used as an external bias to change the surface potential of the gold surface. The gold thin film sample is used in experiment I. The data is collected with a 1 V external bias and with a V_{ac} range from 0.1 to 18 V. The purpose of this experiment is to demonstrate the V_{ac} dependence in SKPM readings and to test the hypothesis that there is a V_{ac} dependent systematic error in the measurement results. In experiment II, the gold surface is biased at 0, 0.2, 0.4, 0.6, 0.8, and 1 V. The V_{ac} range is from 0.2 to 6 V for each bias. The purpose of this experiment is to apply the proposed methodology to recover the CPD from V_{ac} dependent SKPM results. The silicon sample with the thin thermal oxide passivation layer is scanned in experiment III. The purpose of this experiment is to test the theory with a semiconductor based sample. The range of V_{ac} is selected such that it covers small V_{ac} values according to the criterion in Eq. (14). For a silicon substrate with a resistivity of 3–6 Ω cm, $Q_{d_\max}$ is estimated to be between 2×10^{-4} C/m^2 and 3×10^{-4} C/m^2. With a 50 nm tip to sample distance, V_{ac} needs to be smaller than 0.8 V, determined using Eq. (14).

IV. RESULTS AND DISCUSSION

Figure 4 shows the surface topography and the CPD profile of the gold thin film sample measured at three driving amplitudes (V_{ac}=0.1, 1, and 10 V). In Fig. 4(a) the topography of the gold thin film is homogenous, whereas in Fig. 4(b) the measured CPD changes when changing V_{ac}. The CPD profile shown in Fig. 4(b) is scanned with a zero external bias. For 1 V and other bias voltages, the measured CPD profile looks the same except with an offset that equals the bias voltage. Figure 4 demonstrates that the output of the SKPM measurement V_{dc} is a function of the driving amplitude V_{ac}, although the actual contact potential difference between the tip and the gold thin film should remain the same. The magnitude of V_{dc} increases as V_{ac} decreases.

To test our hypothesis that there is an V_{ac} dependent systematic error in the measurement results, the measured V_{dc} in experiment I is plotted as a function of $1/V_{\text{ac}}$ in Fig. 5(a). The sample is biased at 1 V. Figure 5(a) shows that V_{dc}

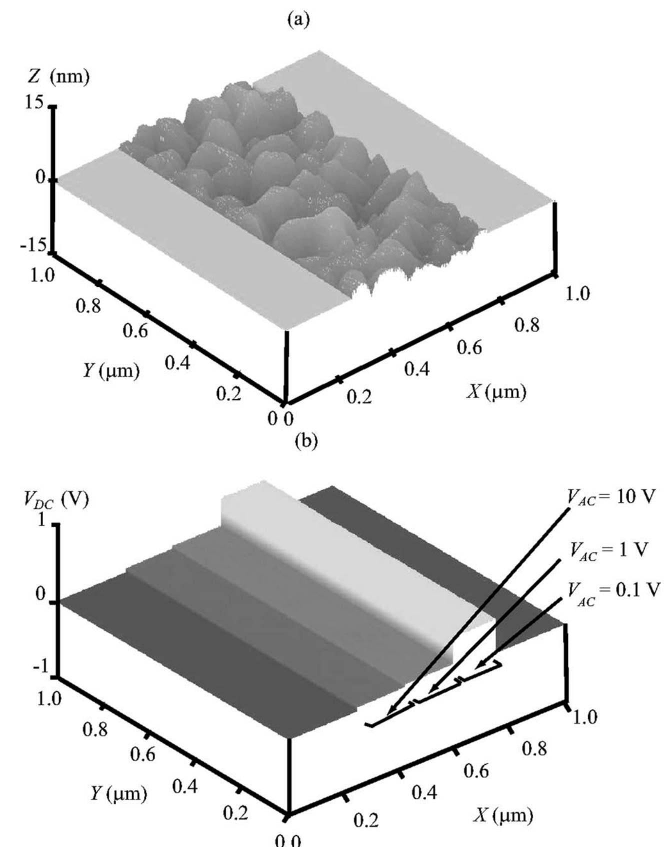

FIG. 4. Topography (a) of the gold thin film sample surface and the contact potential difference (b) between gold and platinum tip measured by SKPM with three driving amplitudes V_{ac} (0.1, 1, and 10 V). The CPD profile shown here is scanned with a zero external bias.

Downloaded 04 May 2006 to 130.126.178.112. Redistribution subject to AIP license or copyright, see http://rsi.aip.org/rsi/copyright.jsp

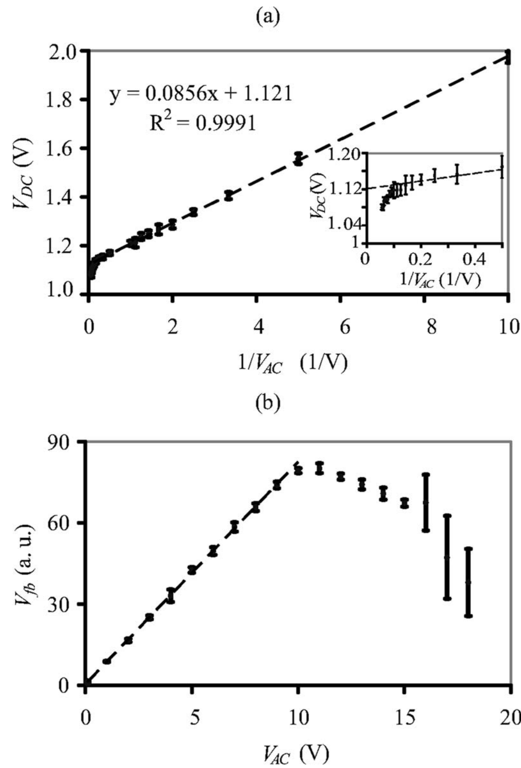

FIG. 5. The SKPM response results for (a) V_{dc} vs $1/V_{ac}$ and (b) V_{fb} vs V_{ac} for the gold thin film sample when the external bias is 1 V. The unit of V_{fb} is recorded as an arbitrary unit since the real units for the V_{fb} data is unavailable for the instrument being used.

is a linear function of $1/V_{ac}$, as Eq. (8) predicts. The V_{ac} dependent systematic error increases as the ac driving amplitude decreases, leading to a greater dependence of V_{ac} in the measurement results. As V_{ac} decreases from 0.5 to 0.1 V ($1/V_{ac}$ increases from 2 to 10 V^{-1}), V_{dc} increases from 1.286 to 1.973 V. When V_{ac} decreases, an increased uncertainty in the measurement results is shown by the longer error bars in Fig. 5(a). This observation agrees with that of Arakawa *et al.*[12] To apply the proposed methodology to recover the true CPD in the measurement results, we need to find out the range over which the feedback signal to the controller V_{fb} is approximately linear with respect to driving amplitude V_{ac}. Figure 5(b) shows V_{fb} as a function of V_{ac}, which increases linearly as V_{ac} increases from 0.1 to 9 V. For V_{ac} greater than 9 V, the slope of the V_{fb} vs V_{ac} curve starts to decrease. This decrease can be due to a change in the θ and g as the dc electrostatic force between the tip and the sample increases. When V_{ac} is greater than 16 V, the V_{fb} signal shows an abrupt increase in variations. The magnitude of V_{fb} follows the surface topography for the range from 16 to 18 V, which indicates that the tip is vibrating in close vicinity to the surface due to the bending of the cantilever. The decrease of slope in the V_{fb} vs V_{ac} data corresponds to the deviation of the linear relationship in the V_{dc} vs $1/V_{ac}$ data, as shown in the inset of Fig. 5(a). When applying the proposed methodology to recover the true CPD, it is important to exclude the data for V_{ac} greater than 9 V since in this region V_{fb} is not linear with respect to the driving amplitude V_{ac}. The linear regression result for the V_{dc} vs $1/V_{ac}$ data for a V_{ac} range of 0.1–9 V is shown in Fig. 5(a). According to Eq. (8), the contact potential difference between the tip and the gold thin film sample will equal the intercept. Within 95% confidence bounds, the intercept is estimated to be 1.121±0.003 V from the experimental data. In this experiment, the external bias voltage determines the surface potential of the sample ϕ_1 in Eq. (2). For a 1 V bias, the work function difference between the conductive coating layer of the tip (platinum-iridium) and the gold is estimated to be 0.121±0.003 eV from this experiment. This value, however, is not consistent with tabulated work function values of polycrystalline gold (5.351 eV), platinum (5.65 eV), and iridium (5.27 eV) under UHV conditions,[21] since the experiments are performed in air.

TABLE II. Linear regression results for V_{dc} vs $1/V_{ac}$ data of experiment II.

Bias (V)	Slope (V^2)	Intercept/CPD (V)	R^2	W_{PtIr}-W_{Au} (eV)
0.000	0.031±0.002	0.066±0.005	0.9710	0.066±0.006
0.200	0.029±0.002	0.253±0.004	0.9837	0.053±0.005
0.400	0.027±0.002	0.470±0.003	0.9849	0.070±0.004
0.600	0.028±0.002	0.660±0.004	0.9823	0.060±0.005
0.800	0.030±0.002	0.867±0.003	0.9861	0.067±0.004
1.000	0.028±0.002	1.062±0.005	0.9630	0.062±0.006

Linear regression results for the data obtained in experiment II with the Au sample are shown in Table II. In this experiment, the work function difference between the tip and the sample is constant, while the surface potential of the gold thin film sample is raised as the external bias increases from 0 to 1 V. Table II shows that the CPD value determined from the intercept increases as the external bias increases. Within 95% confidence bounds, the recovered CPD value corresponds to the bias and the work function difference in each of the six tests in this experiment. The work function difference between the tip (platinum-iridium) and the sample (gold) is calculated by subtracting the bias voltage from the recovered CPD and is listed in the last column of Table II. For this experiment, the work function differences for each bias voltage are estimated to be from 0.053±0.004 eV to 0.070±0.003 eV, giving a single expected value of 0.063±0.008 eV. Compared with the estimated value from experiment I (0.121±0.003 eV), the work function difference is 0.058 eV lower. Potential explanations to account for the discrepancies of the work function difference in experiments I and II include (a) the difference in the tip-sample distance between the two experiments, as shown in Table I (61.6 nm in experiment I and 31.8 nm in experiment II) and (b) the possible change in the relative humidity of the air during the time when the two experiments were conducted. The mechanisms for the dependence in SKPM readings on the tip-sample distance have been studied by Jacobs *et al.*[6] The effect of the potential shielding by a surface water layer in SKPM has been studied by Sugimura *et al.*,[22] and the SKPM measurement results were found to be affected by atmospheric conditions, particularly by the relative humidity of the air due to adsorbed water molecules.

Figure 6(a) and 6(b) show the V_{dc} vs $1/V_{ac}$ response and the V_{fb} vs V_{ac} response for the thermal oxide passivated silicon sample, respectively. For this type of sample, it is pos-

Downloaded 04 May 2006 to 130.126.178.112. Redistribution subject to AIP license or copyright, see http://rsi.aip.org/rsi/copyright.jsp

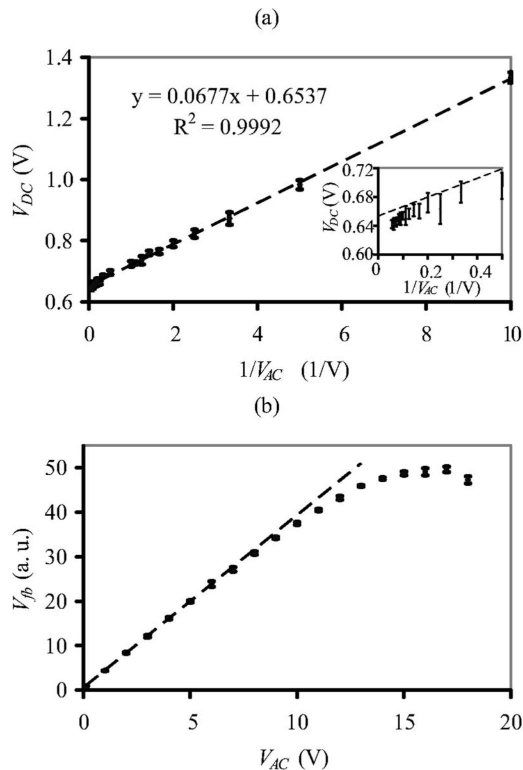

FIG. 6. The SKPM response results for (a) the V_{dc} vs $1/V_{ac}$ response and (b) the V_{fb} vs V_{ac} response for the thermal oxide passivated silicon sample. The unit of V_{fb} is recorded as an arbitrary unit since the real units for the V_{fb} data is unavailable for the instrument being used.

sible for the V_{ac} induced semiconductor surface charge to oscillate and shift the apparent CPD at the same time when the V_{ac} dependent systematic error is present. The V_{ac} range used for applying the linear regression method to recover the true CPD value needs to be small enough to avoid a significant change in V_s that occurs with the alternating electric field. As shown in Sec. III for our case, V_{ac} needs to be smaller than 0.8 V. The linear regression result for the V_{dc} vs $1/V_{ac}$ data for a V_{ac} range of 0.1 to 0.8 V is shown in Fig. 6(a). The recovered CPD value for this set of data is 0.654 ± 0.006 V. The deviation from the linear relationship between V_{dc} and $1/V_{ac}$ in the inset of Fig. 6(a) corresponds to the deviation from the linear relationship between V_{fb} and V_{ac}, when V_{ac} is greater than 10 V in Fig. 6(b). In Fig. 6(b), when V_{ac} is greater than 10 V, the response of V_{fb} starts to drop below the original linear slope. Again, the change of slope can be due to a change in the phase lag θ and the tip-sample distance g as the dc electrostatic force between the tip and the sample increases.

Since V_{fb} no longer increases linearly with V_{ac}, when V_{ac} is greater than 10 V, as indicated in Fig. 6(b), the deviation from the linear relationship between V_{dc} and $1/V_{ac}$ for increasing V_{ac} in the inset of Fig. 6(a) may not be caused by the asymmetric band bending nature of semiconductor surfaces. Moreover, even if the linear regression is applied only to the data range of 0.1–0.8 V ($1.25-10\ V^{-1}$), the rest of the data points in Fig. 6(a) still falls in close vicinity of the straight line as V_{ac} ranges from 1 to 18 V, which suggests that there is no detectable change in V_s due to the space charge response to the alternating electric field inside the silicon substrate. Possible reasons for not detecting the semiconductor surface nature originated V_{ac} dependence with the tested sample include the following (a) the interface state density between the silicon and the thermal oxide may be large enough to block a significant amount of field induced charge to the bulk silicon, and (b) there may be a large amount of fixed charges on the silicon surface such that the silicon surface is in strong inversion or accumulation. The data for the thermal oxide passivated silicon sample shows that V_{ac} dependent SKPM readings due to the asymmetric band bending is not always observable with semiconductor samples, whereas the V_{ac} dependent systematic error is common as long as there is a nonzero tracking error in the control loop. If the V_{ac} dependent systematic error is accounted for in the apparent CPD readings, decreasing V_{ac} will cause an increasing uncertainty in SKPM measurements for semiconductor samples. Thus the application of the proposed methodology to recover the true CPD value when V_{ac} is reduced is still needed to suppress the effect of the asymmetric band bending for semiconductor samples.

V. SUMMARY

We have demonstrated that the tracking error in the feedback loop of the SKPM system can cause an ac amplitude dependent systematic error in SKPM measurements. The main point of this article is that the true contact potential difference can be separated from the ac driving amplitude dependent systematic error in SKPM measurements. To identify the ac driving amplitude dependent systematic error, a measured CPD versus over the inverse ac driving amplitude plot can be used. From this plot, the true contact potential difference can be estimated by SKPM from the intercept on the y axis, along with the uncertainty from the 95% confidence bounds, provided that the feedback signal to the servo controller is linearly proportional to the ac driving amplitude. The systematic error should not be confused with the ac driving amplitude dependent SKPM reading due to the asymmetric band bending nature of semiconductor surfaces, which occurs only for semiconductor samples at particular conditions. When the asymmetric band bending occurs at the same time when the V_{ac} dependent systematic error is present, a smaller V_{ac} reduces the effect of the asymmetric carrier response to a semiconductor surface but leads to a greater V_{ac} dependent systematic error. However, the proposed method to correct for the systematic error allows for true CPD to be estimated for semiconductor materials in these situations.

ACKNOWLEDGMENTS

This work was supported by the *WaterCAMPWS*, a Science and Technology Center of Advanced Materials for the Purification of Water with Systems under the National Science Foundation (NSF) Agreement No. CTS-0120978. Any opinions, findings, and conclusions or recommendations expressed in this publication are those of the authors and do not necessarily reflect the views of NSF. The AFM work was performed at the Center for Microanalysis of Materials, University of Illinois at Urbana-Champaign, partially supported by the U.S. DOE under Grant No. DEFC02-91-ER45439.

Downloaded 04 May 2006 to 130.126.178.112. Redistribution subject to AIP license or copyright, see http://rsi.aip.org/rsi/copyright.jsp

The authors would like to acknowledge Dr. Scott MacLaren for his assistance with the AFM experiments.

[1] M. Nonnenmacher, M.P. O'Boyle, and H. K. Wickramasinghe, Appl. Phys. Lett. **58**, 2921 (1991).
[2] L. Kronik and Y. Shapira, Surf. Sci. Rep. **37**, 1 (1999).
[3] D. K. Schroder, Meas. Sci. Technol. **12**, R16 (2001).
[4] A. K. Henning and T. Hochwitz, Mater. Sci. Eng., B **B42**, 88 (1996).
[5] V. D. Frolov, S. M. Pimenov, V. I. Knonov, V. I. Polyakov, A. I. Rukovishnikov, N. M. Rossukanyi, J. A. Carlisle, and D. M. Gruen, Surf. Interface Anal. **36**, 449 (2004).
[6] H. O. Jacobs, P. Leuchtmann, O. J. Homan, and A. Stemmer, J. Appl. Phys. **84**, 1168 (1998).
[7] O. Vatel and M. Tanimoto, J. Appl. Phys. **77**, 2358 (1995).
[8] R. Shikler and Y. Rosenwaks, Appl. Surf. Sci. **157**, 256 (2000).
[9] H. O. Jacobs, H. F. Knapp, and A. Stemmer, Rev. Sci. Instrum. **70**, 1756 (1999).
[10] Y. Leng and C. C. Williams, Appl. Phys. Lett. **66**, 1264 (1995).
[11] A. K. Henning, Proc. SPIE **3512**, 54 (1998).
[12] M. Arakawa, S. Kishimoto, and T. Mizutani, Jpn. J. Appl. Phys., Part 1 **36**, 1826 (1997).
[13] B. M. Law and F. Rieutord, Phys. Rev. B **66**, 035402 (2002).
[14] S. Hudlet, M. Saint Jean, C. Guthmann, and J. Berger, Eur. Phys. J. B **2**, 5 (1998).
[15] S. Belaidi, P. Girard, and G. Leveque, J. Appl. Phys. **81**, 1023 (1997).
[16] C. G. B. Garrett and W. H. Brattain, Phys. Rev. **99**, 376 (1955).
[17] G. Koley and M. G. Spencer, Appl. Phys. Lett. **79**, 545 (2001).
[18] T. Hochwitz, A. K. Henning, C. Levey, C. Daghlian, and J. Slinkman, J. Vac. Sci. Technol. B **14**, 457 (1996).
[19] T. Matsukawa, S. Kanemar, M. Masahara, M. Nagao, H. Tanoue, and J. Itoh, Appl. Phys. Lett. **82**, 2166 (2003).
[20] *Dimension 3100 manual, Version 4.43B* (Digital Instruments, Veeco Metrology Group, Santa Barbara, CA, 2000).
[21] *Handbook of Chemistry and Physics*, 68th ed. (CRC, Boca Raton, FL, 1986).
[22] H. Sugimura, Y. Ishida, K. Hayashi, O. Takai, and N. Nakagiri, Appl. Phys. Lett. **80**, 1459 (2002).

Downloaded 04 May 2006 to 130.126.178.112. Redistribution subject to AIP license or copyright, see http://rsi.aip.org/rsi/copyright.jsp